Preclinical Activity of HER2-Selective Tyrosine Kinase Inhibitor Tucatinib as a Single Agent or in Combination with Trastuzumab or Docetaxel in Solid Tumor Models AC

Anita Kulukian[1], Patrice Lee[2], Janelle Taylor[1], Robert Rosler[3], Peter de Vries[3], Daniel Watson[1], Andres Forero-Torres[1], and Scott Peterson[1]

ABSTRACT

HER2 is a transmembrane tyrosine kinase receptor that mediates cell growth, differentiation, and survival. HER2 is overexpressed in approximately 20% of breast cancers and in subsets of gastric, colorectal, and esophageal cancers. Both antibody and small-molecule drugs that target HER2 and block its tyrosine kinase activity are effective in treating HER2-driven cancers. In this article, we describe the preclinical properties of tucatinib, an orally available, reversible HER2-targeted small-molecule tyrosine kinase inhibitor. In both biochemical and cell signaling experiments, tucatinib inhibits HER2 kinase activity with single-digit nanomolar potency and provides exceptional selectivity for HER2 compared with the related receptor tyrosine kinase EGFR, with a >1,000-fold enhancement in potency for HER2 in cell signaling assays. Tucatinib potently inhibits signal transduction downstream of HER2 and HER3 through the MAPK and PI3K/AKT pathways and is selectively cytotoxic in HER2-amplified breast cancer cell lines *in vitro*. *In vivo*, tucatinib is active in multiple HER2$^+$ tumor models as a single agent and shows enhanced antitumor activity in combination with trastuzumab or docetaxel, resulting in improved rates of partial and complete tumor regression. These preclinical data, taken together with the phase-I tucatinib clinical trial results demonstrating preliminary safety and activity, establish the unique pharmacologic properties of tucatinib and underscore the rationale for investigating its utility in HER2$^+$ cancers.

Graphical Abstract: http://mct.aacrjournals.org/content/molcanther/19/4/976/F1.large.jpg.

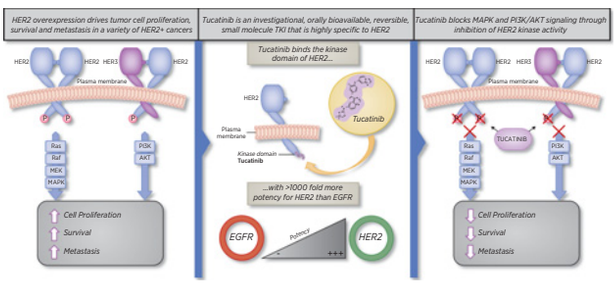

Tucatinib is an investigational agent and its efficacy and safety have not been established

Introduction

HER2 gain-of-function mutations and gene amplification are observed in a subset of carcinomas, including breast, bladder, colorectal, non–small cell lung, esophageal, and gastric cancers (1–5). HER2 amplification, detected by IHC and FISH, has been observed in approximately 20% of invasive breast tumors (6–8), while HER2 overexpression has been observed in 6% to 37% of gastric cancers and 5% of colorectal cancers (9, 10). HER2 is a member of the human EGFR or HER receptor tyrosine kinase (RTK) subfamily, which includes 4 members: EGFR (HER1/erbB1), HER2 (neu/erbB2), HER3 (erbB3), and HER4 (erbB4; ref. 11). These proteins are structurally conserved with an extracellular ligand-binding domain, a transmembrane domain, and an intracellular kinase domain.

The activity of these receptors in tissues is regulated by ligand binding, which drives receptor dimerization (homodimers or heterodimers) and elicitation of downstream signaling via the activation of the C-terminal tyrosine kinase domain (2, 3). Although HER family proteins are structurally similar, HER2 lacks a ligand-binding site on its extracellular domain and has no known activating ligand, while HER3 displays extremely low or nonexistent protein kinase activity (11). As such, both HER2 and HER3 rely upon dimerization partners for active signaling, often forming heterodimers with each other (2, 3). Activation of the kinase activity of the HER RTKs results in the transphosphorylation of intracellular domains within homodimeric or heterodimeric complexes, leading to the scaffolding of adaptor protein networks and stimulation of downstream effectors, including activation of the MAPK and PI3K pathways (2, 3). HER2 is the preferred dimerization partner with other EGFR subfamily members, such as HER3, and subverts cellular signaling when overexpressed in tumor cells, resulting in constitutive activation of mitogenic and prosurvival signaling (2, 3, 12–14).

Significant progress has been made in treating HER2$^+$ disease, particularly in breast cancer where multiple HER2-targeted drugs have been developed that have significantly prolonged the life of patients, particularly those with early-stage HER2$^+$ breast cancer (3, 10, 15–18). However, up to a quarter of all patients treated with anti-HER2 therapy in the adjuvant setting relapse (15–18), underscoring the need for new drugs designed to treat HER2-driven malignancies in the later-stage setting. Currently, approved treatments for patients with HER2$^+$ breast cancer include mAb therapies, such as trastuzumab and

[1]Seattle Genetics, Bothell, Washington. [2]Array Biopharma, Boulder, Colorado. [3]Cascadian Therapeutics, Seattle, Washington.

Note: Supplementary data for this article are available at Molecular Cancer Therapeutics Online (http://mct.aacrjournals.org/).

Current address for R. Rosler: Celgene, Inc., Summit, New Jersey; and current address for P. de Vries, ApoGen Biotechnologies, Seattle, Washington.

Corresponding Author: Scott Peterson, Seattle Genetics, 21823 30th Dr. SE, Bothell, WA 98021. Phone: 425-527-2788; Fax: 425-527-4109; E-mail: speterson@seagen.com

Mol Cancer Ther 2020;19:976–87

doi: 10.1158/1535-7163.MCT-19-0873

©2020 American Association for Cancer Research.

Downloaded from http://aacrjournals.org/mct/article-pdf/19/4/976/1848445/976.pdf by guest on 19 May 2025

pertuzumab, the antibody–drug conjugate adotrastuzumab emtansine, and the small-molecule tyrosine kinase inhibitors (TKI) lapatinib and neratinib (3, 19–21). Both lapatinib and neratinib demonstrate nearly equipotent inhibition of EGFR and HER2 (22, 23), which is thought to contribute to high frequencies of dermatologic and gastrointestinal adverse events (AE), necessitating dose interruptions and modifications (24, 25).

Considering the tolerability challenges imposed by the potent coinhibition of HER2 and EGFR by the approved HER2-targeted TKIs lapatinib and neratinib, there is an unmet need for novel TKIs that inhibit HER2 activity while sparing other EGFR subfamily proteins to facilitate dosing continuity, maintain efficacy, and increase tolerability. In this article, we provide a preclinical characterization of tucatinib, an orally bioavailable, small-molecule HER2-targeted TKI that has shown clinical activity in studies of HER2$^+$ advanced cancers, including activity in brain metastases (19, 26–47).

Materials and Methods

Biochemical assays

HER2 biochemical assays were performed using HER2 aa 679–1255 produced as an N-terminal GST fusion protein (Proquinase #015). Assays contained 16.7 nmol/L HER2 enzyme and 0.2 μg/mL poly (Glu-Tyr) E4Y1 peptide substrate (Sigma). Assays were performed in 50 mmol/L HEPES, pH 7.5, 20 mmol/L $MgCl_2$, 0.5 mmol/L DTT, and 0.01% Tween using 22 μmol/L ATP. Kinase activity was determined after 4-hour incubation at 25°C using ADP-Glo reagent (Promega). EGFR biochemical assays were performed using EGFR aa 668–1091 produced as an N-terminal GST fusion protein (SignalChem #E10-112G). Assays contained 6 nmol/L enzyme and 0.2 μg/mL substrate peptide poly (Glu-Tyr), E4Y1. Assays were performed in 50 mmol/L HEPES, pH 7.5, 20 mmol/L $MgCl_2$, 5 mmol/L $MnCl_2$, 0.5 mmol/L DTT, and 0.01% Tween using 14.8 μmol/L ATP. Kinase activity was determined after 2-hour incubation at 25°C using ADP-Glo reagent.

IC_{50} values for kinase activity inhibition were determined by fitting ADP-Glo assay data using a nonlinear 4-parameter variable slope formula (GraphPad Prism). Tucatinib potency was determined using data from a 12-point serial dilution (3-fold dilutions) of drug ranging from 0.00017 to 30 μmol/L. Neratinib potency was determined using data from a 12-point serial dilution (3-fold dilutions) of drug ranging from 0.0000339 to 6 μmol/L. Lapatinib potency was determined using data from a 16-point serial dilution (2-fold dilutions) of drug ranging from 0.000137 to 4.5 μmol/L.

The HER4 kinase assay was performed using N-terminal His6-tagged recombinant human ErbB4 (aa 706–991 expressed by baculovirus) and 7.5 μmol/L ATP in assay buffer [50 mmol/L HEPES, pH 7.3, 5 mmol/L $MgCl_2$, 0.2 mmol/L $MnCl_2$, 0.1 mmol/L Na_3VO_4, final DMSO concentration 1% (v/v)]. Reagents were incubated on 0.25 mg/mL PGT-coated plates for 20 minutes at room temperature. The reaction mixture was removed by washing and the phosphorylated polymer substrate was detected with 0.2 μg/mL phosphotyrosine specific mAb (PY20) conjugated to horseradish peroxidase. After the addition of 1 mol/L phosphoric acid to stop the development, the chromogenic substrate color was quantified by spectrophotometry at 450 nm. IC_{50} values were determined by fitting data using a nonlinear 4-parameter variable slope formula (GraphPad Prism). Tucatinib potency in the HER4 assay was determined using data from a 10-point serial dilution (3-fold dilutions) of drug ranging from 0.000508 to 10 μmol/L.

Kinase-inhibitory activity profiling screen

Tucatinib-inhibitory activity against 223 kinases was analyzed using the KinaseProfiler service (Millipore). Compounds were run in duplicate at a concentration of ATP near the K_m for each individual kinase according to the manufacturer's specifications. Tucatinib activity across this panel of kinases is represented by a kinome tree illustration (Cell Signaling Technology), which was created using the KinMap web-based tool (www.kinhub.org/kinmap; ref. 29). Tucatinib activity was assessed at 1 and 10 μmol/L.

Phosphorylation analysis

HER2 and EGFR

BT-474 and A431 cells (1.5×10^5 cells in a 24-well) were seeded overnight and treated with increasing concentrations of tucatinib (0.1–10,000 nmol/L) per well for 2 hours. Samples were run with two replicates. Purified EGF (Cell Signaling Technology) was added to A431 cells for a final concentration of 10 ng/mL for 10 minutes prior to harvest. Lysates were prepared with buffer (supplied) containing protease and phosphatase inhibitors, and samples were processed using PathScan Sandwich ELISA kit (Cell Signaling Technology) according to manufacturer's protocol. Assays were performed for total HER2 (Cell Signaling Technology, catalog no. 7310), phospho-HER2 (pan-Tyr, Cell Signaling Technology, catalog no. 7968), total EGFR (Cell Signaling Technology, catalog no. 7250), and phospho-EGFR (pan-Tyr, Cell Signaling Technology, catalog no. 7911). Phosphorylated protein levels were normalized to total protein levels. Analysis was performed within GraphPad Prism software, with IC_{50} values generated from best-fit curves log(inhibitor) versus response—4-parameter variable slope formula. Errors bars represent SD.

HER2, HER3, MEK, ERK, and AKT phosphorylation assays

BT-474 cells (30,000 per 96-well) were seeded overnight and treated with increasing concentrations of tucatinib for 2 hours at 37°C. Lysates were collected and phosphorylation of respective proteins was analyzed with phospho-ERK 1/2, phospho-MEK1, and phospho-AKT MapMate kits (Millipore) while phospho-HER2 and phospho-HER3 were detected by a custom phospho-RTK panel (Millipore) according to the manufacturer's protocol. Samples were run on a Luminex LX200 instrument (R&D Systems) using xPONENT software.

Cell lines

BT474 and A431 cells were obtained from ATCC in 2018 and 2013, respectively. Cell lines were demonstrated to be free of *Mycoplasma* by PCR evaluation and were authenticated by marker analysis prior to banking (completed by Idexx Bioanalytics). Cells were maintained in culture for a maximum of 7 weeks (7–15 passages).

Quantitative flow cytometry analysis of cell surface receptor density

HER2 and EGFR cell surface levels were determined using quantitative flow cytometry–based Qifi kit (Agilent Dako, catalog no. K0078) executed according to manufacturer's protocol. Cells were stained with anti-HER2 antibody (R&D Systems, catalog no. MAB1129) and anti-EGFR antibody (Abcam, catalog no. ab30) for quantification.

Cytotoxicity assays

BT-474 (4,000 cells per 96-well) and A431 (5,000 cells per 96-well) cells were seeded overnight in duplicate and treated with increasing concentrations of tucatinib (0.15–10,000 nmol/L). Cell viability was measured at 96 hours using a CellTiter-Glo (CTG) Luminescent Cell

Downloaded from http://aacrjournals.org/mct/article-pdf/19/4/976/1848445/976.pdf by guest on 19 May 2025

Viability assay (Promega) following manufacturer's protocol. Data were analyzed in GraphPad Prism, and EC_{50} values were generated from best-fit curves. Cytotoxicity against the panel of breast cancer cell lines were run in similar format and are described in greater detail in Supplementary Methods.

Caspase-3/7 apoptosis assays

BT-474 cells (50,000 per well) were seeded overnight and then treated with increasing concentrations of tucatinib (0.2–1,000 nmol/L) and trastuzumab (150 μg/mL; equivalent to 1 μmol/L) for 18 hours at 37°C. Caspase-Glo 3/7 reagent and buffer (100 μL/well) was added and after 30-minute incubation, caspase-3/7 activity was quantified on a BMG PolarSTAR Luminator (BMG LABTECH).

Xenograft models

Cell line–derived (CDX) breast (BT-474) and gastric (NCI-N87) cancer cells were implanted subcutaneously into the flanks of female immunocompromised mice. Animals were treated with tucatinib (25, 50, or 100 mg/kg orally, every day), trastuzumab (20 mg/kg, intraperitoneally, every 3 days), docetaxel (10 mg/kg, intravenously, once weekly), or vehicle (30% Captisol, orally, everyday). Patient-derived (PDX) tumor fragments from solid tumors (breast, gastric, colorectal, and esophageal) were implanted subcutaneously into the flanks of immunocompromised mice. Mice were treated with tucatinib (50 mg/kg, orally, twice a day), trastuzumab (20 mg/kg, intraperitoneally, every 3 days or once weekly), tucatinib + trastuzumab, or vehicles (30% Captisol, orally, every day; PBS, intraperitoneally, twice a week). Animals were followed to the designated end of each experiment. Additional details are described in the Supplementary Methods. All *in vivo* studies adhered to Institutional Animal Care and Use Committee guidelines.

Statistical analysis

Data in xenograft studies are expressed as the mean ± SE. Statistical analyses were performed using data up to the last day that tumor volumes were measured for all groups. Statistical comparisons of tumor volumes in the efficacy studies were conducted using one-way ANOVA followed by Tukey multiple comparisons test to compare between all groups.

Tucatinib preparation

4-([1,2,4]triazolo[1,5-a]pyridin-7-yloxy)-3-methylaniline was prepared at Array Biopharma or Cascadian Therapeutics according to the following process description: step 1: 2-Amino-4-hydroxy pyridine Hydrochloride is treated in a stepwise fashion with N,N-dimethylformamide dimethyl acetal followed by hydroxylamine hydrochloride in dimethylformamide (DMF). The pH is adjusted with 2 mol/L sodium hydroxide solution and water is added to yield (Z)-N-hydroxy-N'-(4-hydroxypyridin-2-yl) formimidamide (85%). Step 2: (Z)-N-hydroxy-N'-(4-hydroxypyridin-2-yl) formimidamide is treated with trifluoroacetic anhydride in dichloromethane at reflux. 6N HCL in isopropyl alcohol (IPA) is charged at room temperature to provide [1,2,4]triazolo[1,5-a]pyridin-7-ol hydrochloride (81%). Step 3: [1,2,4]triazolo[1,5-a]pyridin-7-ol hydrochloride is reacted with 1-fluoro-2-methyl-4-nibrobenzene with potassium carbonate in dimethylformamide at 83°C. Water is charged to yield 7-(2-methyl-4-nitrophenoxy)-[1,2,4]triazolo[1,5-a]pyridine (93%). Step 4: 7-(2-methyl-4-nitrophenoxy)-[1,2,4]triazolo[1,5-a]pyridine is hydrogenated over 5% Pd/C in tetrahydrofuran (THF) at 45°C. Solvent swap to Heptane is performed to yield 4-([1,2,4]triazolo[1,5-a]pyridin-7-yloxy)-3-methylaniline (94%).

(E)-N′-(2-Cyano-4-(3-(1-hydroxy-2-methylpropan-2-yl)thioureido)phenyl)-N,N-dimethylformimidamide was synthesized according to the following process description. Step 1: 2-amino-5-nitrobenzonitrile is treated with N,N-dimethylformamide dimethyl acetal in a mixture of methanol and methyl-tert-butyl ether at 40°C to yield (E)-N'-(2-cyano-4-nitrophenyl)-N,N-dimethylformimidamide (95%). Step 2: (E)-N'-(2-cyano-4-nitrophenyl)-N,N-dimethylformimidamide in THF is hydrogenated with 10% Pd/C at 35°C. Solvent swap to IPA is performed to provide (E)-N'-(4-amino-2-cyanophenyl)-N,N-dimethylformimidamide (90%). Step 3: (E)-N'-(4-amino-2-cyanophenyl)-N,N-dimethylformimidamide in THF is charged to a solution of 1,1-thiocarbonyldiimidazole in THF at -14°C. 2-amino-2-methyl-1-propanol in THF is charged and then the solvent is swapped to IPA to isolate (E)-N′-(2-Cyano-4-(3-(1-hydroxy-2-methylpropan-2-yl)thioureido)phenyl)-N,N-dimethylformimidamide (80%)

Tucatinib, (N4-(4-([1,2,4]triazolo[1,5-α]pyridin-7-yloxy)-3-methylphenyl)-N6-(4,4-dimethyl-4,5-dihydrooxazol-2-yl)quinazoline-4,6-diamine) was synthesized according to the processes described in the United States Patent Application Number US20170136022A1. Step 1: (E)-N′-(2-Cyano-4-(3-(1-hydroxy-2-methylpropan-2-yl) thioureido)phenyl)-N,N-dimethylformimidamide was coupled with 4-([1,2,4]triazolo[1,5-α]pyridin-7-yloxy)-3-methylaniline in isopropyl acetate:acetic acid at 45 °C to yield 1-(4-((4-([1,2,4]triazolo[1,5-α]pyridin-7-yloxy)-3-methylphenyl)amino)quinazolin-6-yl)-3-(1-hydroxy-2-methylpropan-2-yl)thiourea (85%). Step 2: 1-(4-((4-([1,2,4]Triazolo[1,5-α]pyridin-7-yloxy)-3-methylphenyl) amino) quinazolin-6-yl)-3-(1-hydroxy-2-methylpropan-2-yl)thiourea was agitated in THF under basic conditions (2.5 N NaOH), followed by the addition of p-toluenesulfonyl chloride. Water was charged to yield N4-(4-([1,2,4]triazolo[1,5-α]pyridin-7-yloxy)-3-methylphenyl)-N6-(4,4-dimethyl-4,5-dihydrooxazol-2-yl)quinazoline-4, 6-diamine (92%). N4-(4-([1,2,4]Triazolo[1,5-α]pyridin-7-yloxy)-3-methylphenyl)-N6-(4,4-dimethyl-4,5-dihydrooxazol-2-yl)quinazoline- 4,6-diamine was triturated in ethanol at greater than 65°C to provide N4-(4-([1,2,4]triazolo[1,5-α]pyridin-7-yloxy)-3-methylphenyl)-N6-(4,4-dimethyl-4,5-dihydrooxazol-2-yl)quinazoline-4,6-diamine hemi-ethanolate (83%).

Material used in tumor models was manufactured to GMP specifications. MS(ESI): m/z 481 ($M + H^+$); 1HNMR (DMSO-d_6) δ (ppm) 1.31 (s, 6H), 2.21 (s, 3H), 4.08 (s, 2H), 6.83 (d, 2.59 Hz, 1H), 7.00 (dd, 7.43, 2.59 Hz, 1H), 7.67 (d, 1H), 7.67 (s, br (1H), 7.18 (d, 8.73 Hz, 1H), 7.87 (d, 8.73 Hz, 1H), 7.91 (s, 1H), 8.03 (s, br, 1H), 8.35 (s, 1H), 8.5 (s, 1H), 8.89 (d, 1H), 9.15 (s, 1H). 13CNMR (DMSO-d_6) δ (ppm) 16.5 (CH3), 27.3 (2CH3), 56.6 (C), 78.3 (CH2), 98.2 (Ar-C), 108.0 (Ar-C), 116.4 (Ar-C), 121.9 (Ar-C), 122.1 (Ar-C), 125.6 (Ar-C), 128.7 (Ar-C), 130.4 (Ar-C), 131.1 (Ar-C), 138.1 (Ar-C), 146.1 (Ar-C), 147.9 (Ar-C), 151.9 (Ar-C), 152.8 (Ar-C), 155.2 (Ar-C), 156.3 (C), 157.6 (Ar-C), 160.4 (Ar-C). HPLC purity 99.67%.

Results

Tucatinib is a potent and selective HER2 kinase inhibitor

Tucatinib was initially identified via a small-molecule discovery effort focused on HER2 and EGFR TKIs. On the basis of its chemical structure, which is conserved with other TKIs that contain a quinazoline core including lapatinib, erlotinib, and gefitinib (**Fig. 1A**), tucatinib is expected to bind to the ATP pocket of HER2 as a competitive, reversible inhibitor. However, unlike the related HER2-targeted TKI lapatinib (23), tucatinib demonstrates selectivity for HER2 compared with EGFR. In a kinase assay, the half maximal inhibitory constant

Downloaded from http://aacrjournals.org/mct/article-pdf/19/4/976/1848445/976.pdf by guest on 19 May 2025

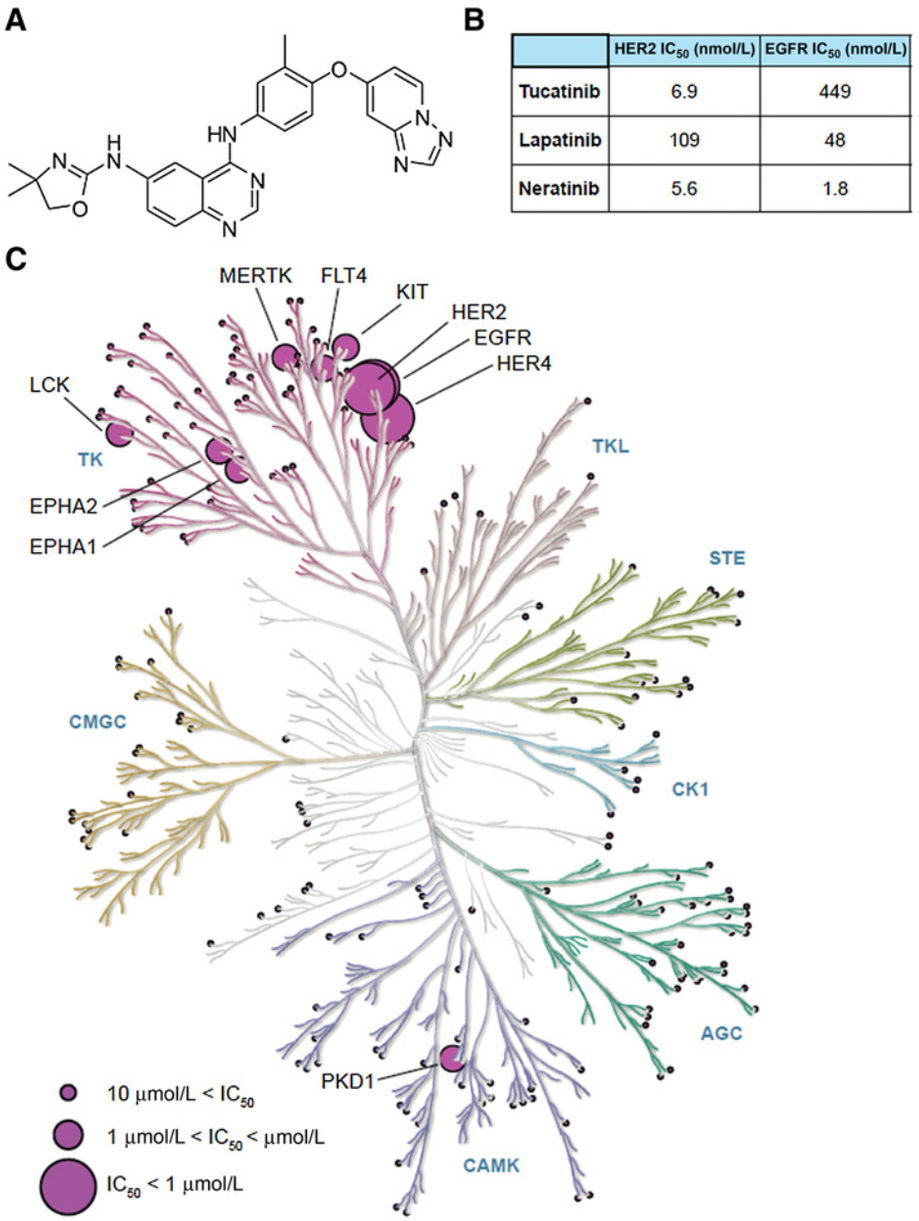

Figure 1.
Enzymatic and kinase screening assays reveal tucatinib potency and selectivity for HER2. **A,** Chemical structure of tucatinib. **B,** Calculated IC_{50} values for tucatinib, lapatinib, and neratinib in a kinase assay using recombinant HER2 and EGFR. **C,** Tucatinib inhibitory activity across a screen of 223 kinases, represented on a kinome dendrogram. Large circles represent kinases inhibited ≥ 50% at 1 µmol/L tucatinib, medium circles represent kinases inhibited ≥ 50% at 10 µmol/L tucatinib, and small circles represent kinases that did not reach 50% inhibition at 10 µmol/L. Illustration reproduced courtesy of Cell Signaling Technology, Inc. (www.cellsignal.com).

(IC_{50}) of tucatinib with HER2 was 6.9 nmol/L, >50-fold lower than that for EGFR, which showed an IC_{50} of 449 nmol/L (**Fig. 1B**). Similarly, tucatinib demonstrated reduced potency in a HER4 biochemical assay relative to HER2, with an IC_{50} of 310 nmol/L. Consistent with published data (22, 23), the IC_{50} values for lapatinib and neratinib for HER2 and EGFR did not show HER2-selective kinase inhibition (**Fig. 1B**). A biochemical screen of 223 kinases confirmed tucatinib selectivity within the EGFR kinase family, with minimal inhibition of other kinases (**Fig. 1C**). Inhibition of non-EGFR kinases in the screen was limited with no kinase demonstrating more than 50% inhibition at a concentration of 1 µmol/L tucatinib and 7 kinases (KIT, EphA1, EphA2, Flt4, Lck, MERTK, PKD1) demonstrating more than 50% inhibition at a concentration of 10 µmol/L tucatinib.

Tucatinib selectively inhibits HER2 signaling activity and cell proliferation in HER2-driven breast cancer cell lines

To determine the potency of tucatinib in blocking HER2 phosphorylation in tumor cells, phosphorylation assays were performed *in vitro* using BT-474 (breast cancer) and A431 (skin cancer) cells. These cell lines were chosen for evaluating tucatinib's cellular HER2 and EGFR activity based on the observation that BT-474 cells due to genomic amplification of the *HER2* gene, resulting in high-level expression of HER2 protein on the cell surface (30), and that A431 cells overexpress EGFR due to genomic amplification of the *EGFR* gene (31). We confirmed these results by measuring the cell surface density of HER2 and EGFR using quantitative flow cytometry (**Fig. 2A**; Supplementary Table S1). In cell signaling assays, tucatinib potently inhibited phosphorylation of HER2 in BT-474 cells (IC_{50} = 7 nmol/L)

Downloaded from http://aacrjournals.org/mct/article-pdf/19/4/976/1848445/976.pdf by guest on 19 May 2025

A

Cell line	HER2 Expression (Molecules)	EGFR Expression (Molecules)
BT-474	864,064	110
A431	6,498	322,832

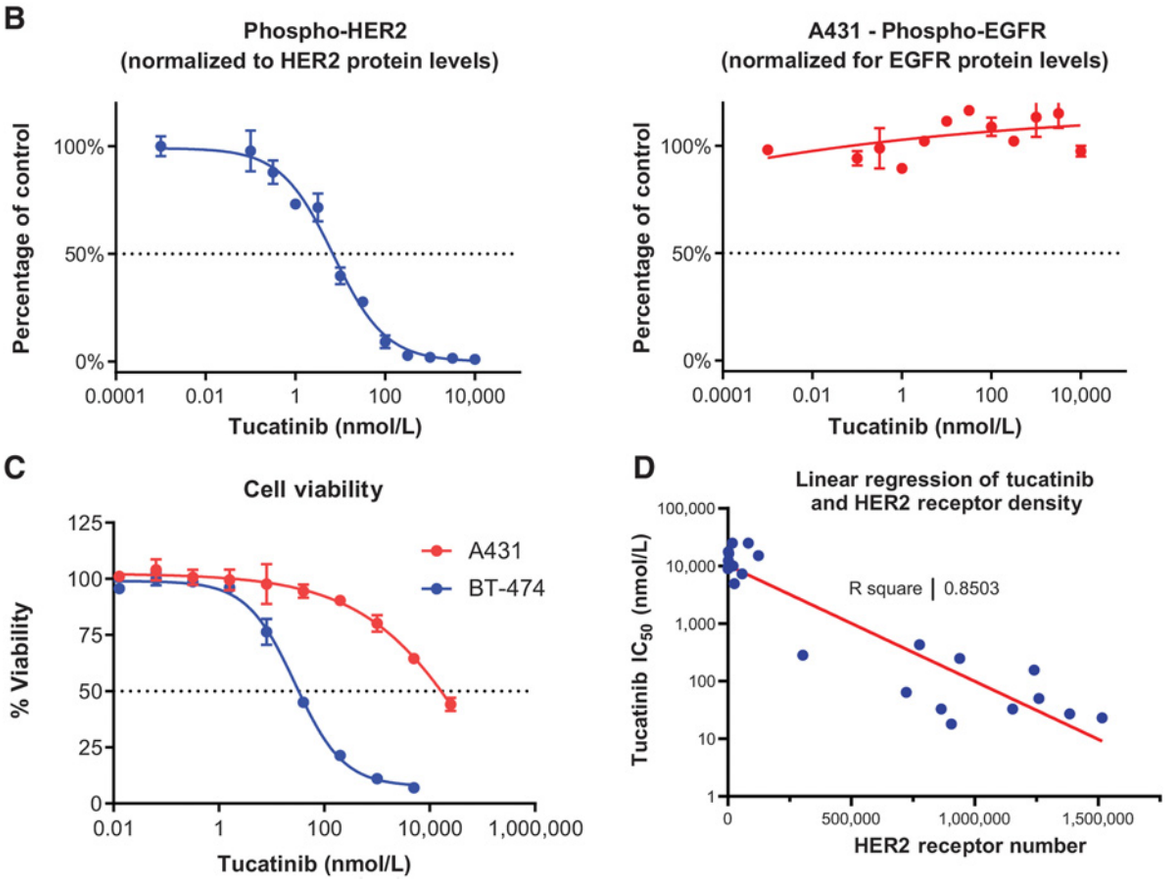

Figure 2.

Tucatinib selectively inhibits HER2-mediated signal transduction and is selectively cytotoxic in HER2-amplified cells. **A,** Surface expression of HER2 and EGFR receptors in BT-471 and A431 cell lines was assessed by quantitative flow cytometry. **B,** Inhibition of HER2 and EGFR by tucatinib in BT-474 and A431 tumor–derived cell lines. Duplicate samples were analyzed by ELISA recognizing a protein or phospho-specific protein (anti-HER2, anti–phospho-HER2, anti-EGFR, anti–phospho-EGFR). Results are expressed as total phospho-protein signal normalized to total protein ± SD. **C,** Cytotoxicity of tucatinib in HER2- (BT-474) and EGFR-amplified (A431) cell lines. Cell viability (± SD) was measured from duplicate samples after 96 hours using the Cell Titer Glo Luminescent Cell Viability Assay. **D,** Comparison of cellular IC_{50} and HER2 expression in breast cancer cell lines. HER2 expression levels were quantified in a panel of 22 breast cancer cell lines using quantitative flow cytometry. IC_{50} values were calculated for each cell line using a 10-point titration of tucatinib. Cell viability was measured after 96 hours using the CellTiter-Glo Luminescent Cell Viability Assay.

but showed minimal inhibition of EGFR phosphorylation in A431 cells (IC_{50} > 10,000 nmol/L; **Fig. 2B**). Tucatinib treatment also strongly inhibited BT-474 cell proliferation (IC_{50} = 33 nmol/L) but had a much less potent effect on A431 cell proliferation, exhibiting an IC_{50} value nearly 500-fold higher (IC_{50} = 16,471 nmol/L; **Fig. 2C**). Similarly, tucatinib showed minimal activity in HER2-negative breast cancer cell lines (IC_{50} range, 4,938 to >25,000 nmol/L), whereas it demonstrated exponentially increasing potency in $HER2^+$ breast cancer cell lines as HER2 surface receptor density increased (IC_{50} range, 23–431 nmol/L; **Fig. 2D**; Supplementary Table S1).

When compared directly with lapatinib or neratinib, only tucatinib demonstrated selectivity for HER2 compared with EGFR (Supplementary Fig. S1). In BT-474 cells, tucatinib inhibited HER2 phosphorylation with an IC_{50} of 7 nmol/L, which was similar to neratinib (IC_{50} = 2 nmol/L) and more potent than lapatinib (IC_{50} = 46 nmol/L; Supplementary Fig. S1). In contrast, tucatinib showed no appreciable inhibition of EGFR phosphorylation in A431 cells when dosed up to 1,000 nmol/L, whereas both neratinib (IC_{50} = 21 nmol/L) and lapatinib (IC_{50} = 36 nmol/L) potently inhibited EGFR phosphorylation (Supplementary Fig. S1). Similarly, in NCI-N87 $HER2^+$ gastric

Downloaded from http://aacrjournals.org/mct/article-pdf/19/4/976/1848445/976.pdf by guest on 19 May 2025

cancer cells, tucatinib potently inhibited HER2 phosphorylation (IC_{50} = 4 nmol/L) but produced only a modest reduction in EGFR phosphorylation at 1,000 nmol/L. In contrast, lapatinib and neratinib both inhibited HER2 and EGFR phosphorylation in NCI-N87 cells with IC_{50} values of 40 and 12 nmol/L, respectively.

Tucatinib + trastuzumab combinations show enhanced inhibition of HER2 signaling activity

HER2 signaling is mediated through activation of other EGFR subfamily members and several downstream effector pathways including MAPK/ERK and PI3K-AKT (12). Treatment of BT-474 cells with tucatinib inhibited phosphorylation of both HER2 and HER3 (**Figs. 2B** and **3A**), a preferred dimerization partner of HER2 (2, 6). In addition, treatment of BT-474 cells with tucatinib inhibited phosphorylation of the downstream effector proteins MEK1 (S222), ERK1/2 (T185/Y187), and AKT (S473; **Fig. 3A**) with IC_{50} values in the same range as HER2 inhibition. Trastuzumab binds to the extracellular domain of HER2, resulting in the inhibition of HER2/HER2 homodimerization, inhibition of downstream signaling through the PI3K–AKT pathway, and suppression of tumor cell proliferation (3, 32). On the basis of differing mechanisms of action by which each treatment inhibits HER2, we hypothesized that combination treatment of tucatinib + trastuzumab may lead to enhanced inhibition of HER2 downstream signaling activity. Treatment of BT-474 cells with tucatinib alone resulted in a dose-dependent reduction of AKT phosphorylation. Treatment of BT-474 cells with 150 μg/mL trastuzumab alone also reduced AKT phosphorylation, and when combined with increasing concentrations of tucatinib, resulted in further diminution of AKT phosphorylation (**Fig. 3B**). Consistent with increased inhibition of AKT phosphorylation, the combination of tucatinib + trastuzumab resulted in a 2-fold increase in caspase-3/7 activity (**Fig. 3C**). Overall, the above data show that tucatinib is a highly selective and potent HER2 inhibitor with strong anticancer cellular effects that are enhanced by combination treatment with trastuzumab.

Tucatinib exhibits activity alone or in combination with trastuzumab or docetaxel in CDX xenograft models of HER2$^+$ cancer

We investigated the ability of tucatinib to prevent tumor cell growth *in vivo* in HER2$^+$ breast and gastric cancer CDX xenograft models. Female immunocompromised mice implanted with BT-474 cells were treated with tucatinib and evaluated for response. Mice treated with tucatinib exhibited tumor growth delay at doses of 25 or 50 mg/kg tucatinib administered orally every day. This effect was similar to mice

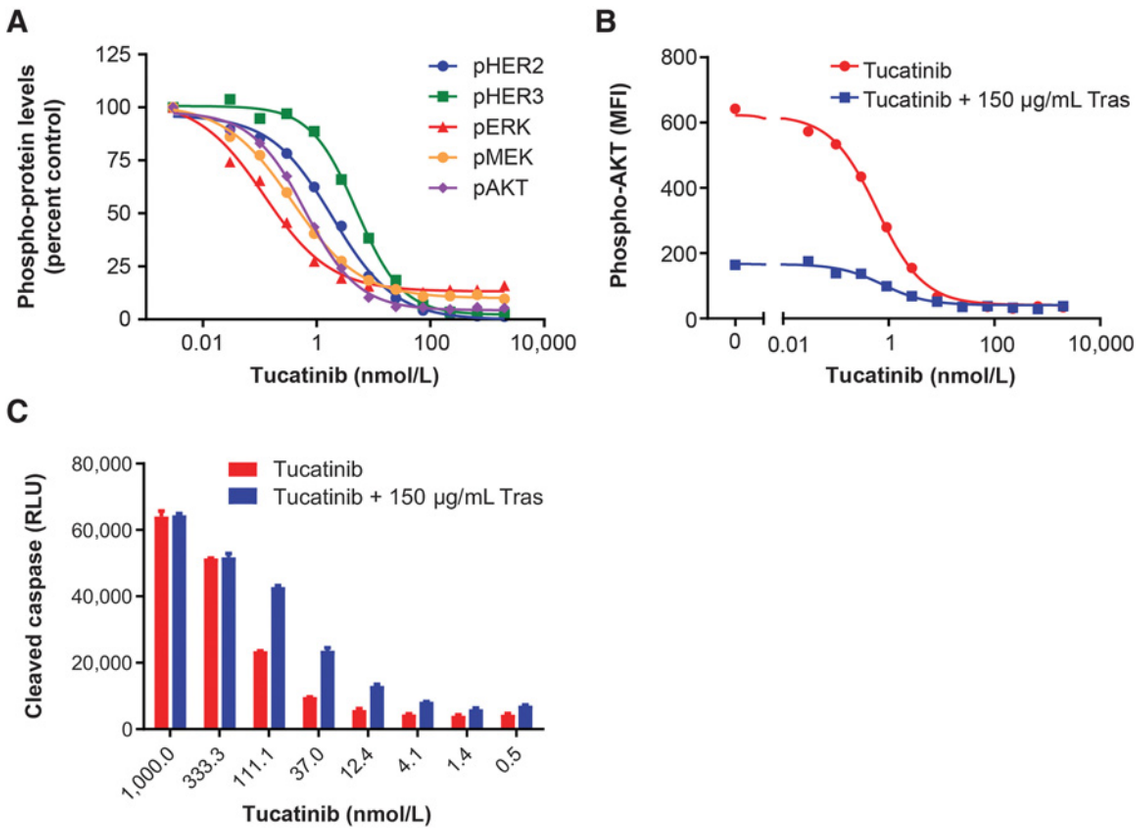

Figure 3.

Tucatinib + trastuzumab additively inhibit HER2 signaling activity and induce apoptosis in HER2-driven breast cancer cell line. **A,** Inhibition of HER2 and HER2 effector signaling. Phosphorylation of target proteins, including total tyrosine phosphorylated HER2 or HER3, phospho-ERK1/2 (T185/Y187), phospho-MEK1 (S222), and phospho-AKT (S473) was quantified. **B,** Additive inhibition of HER2 with tucatinib + trastuzumab (Tras) combination. Phosphorylation of phospho-AKT (S473) was quantified in BT-474 cells treated with tucatinib or tucatinib + trastuzumab and reported as mean fluorescence units (MFI). **C,** Tucatinib- and trastuzumab-mediated apoptosis. Caspase-3/7 activity was quantified from duplicate samples using the Caspase-Glo assay in BT-474 cells treated with tucatinib or tucatinib + trastuzumab and reported as relative light units (RLU) ± SEM.

Downloaded from http://aacrjournals.org/mct/article-pdf/19/4/976/1848445/976.pdf by guest on 19 May 2025

treated with trastuzumab monotherapy (**Fig. 4A**). In contrast, mean tumor volume (MTV) increased > 4-fold in mice treated with vehicle (**Fig. 4A**).

We then investigated the activity of tucatinib combined with docetaxel, a cytotoxic microtubule-targeted drug commonly used in patients with metastatic breast cancer (MBC; ref. 33). Using the BT-474 model, tumor-bearing mice treated with docetaxel exhibited tumor growth delay compared with the vehicle group. Mice treated with tucatinib monotherapy exhibited a similar reduction in tumor growth (**Fig. 4B**). When combined, tucatinib + docetaxel were significantly more active than either drug alone ($P < 0.0001$; **Fig. 4B**).

Given that tucatinib and trastuzumab were both individually effective at reducing tumor growth as single agents in the BT-474 breast cancer model (**Fig. 4A**), we next investigated whether tucatinib + trastuzumab would result in further tumor growth inhibition compared with monotherapy with either agent alone. In an independent experiment, tucatinib monotherapy again resulted in tumor growth inhibition that was similar to trastuzumab monotherapy (**Fig. 4C**). The combination of tucatinib + trastuzumab exhibited enhanced antitumor effects (**Fig. 4C**), resulting in 10 complete tumor regressions and 1 partial tumor regression in the group of 12 treated mice (**Fig. 4C**; **Table 1**). The treatment effect of the combination of tucatinib and trastuzumab was significant when compared with tucatinib alone ($P < 0.0001$) or trastuzumab alone ($P < 0.0001$). Overall, these data suggest that tucatinib is active against HER2$^+$ breast tumors as both monotherapy and in combination with two standard-of-care therapies.

In addition to the BT-474 model, tucatinib was also evaluated in an NCI-N87 HER2$^+$ gastric cancer cell line tumor model. In immunocompromised mice implanted with NCI-N87 cells, tumor growth was inhibited by tucatinib and included 4 partial tumor regressions (**Fig. 4D**). Mice treated with trastuzumab also exhibited a reduction in tumor growth, but no partial regressions (**Fig. 4D**). Mice treated with tucatinib + trastuzumab had an even greater antitumor response with higher rates of tumor regression noted (**Fig. 4D**; **Table 1**). These results were significant when compared with either tucatinib alone ($P = 0.0015$) or compared with trastuzumab alone ($P < 0.0001$). Collectively, these data suggest that tucatinib, alone and in combination with trastuzumab, effectively decreases *in vivo* tumor growth in the NCI-N87 gastric cancer model.

Tucatinib exhibits *in vivo* activity alone or in combination with trastuzumab in HER2$^+$ PDX models of breast, gastric, colorectal, and esophageal cancer

To further investigate the preclinical efficacy of tucatinib, PDX models of HER2$^+$ solid tumors derived from breast, gastric, colorectal, and esophageal cancers were tested. For each model, PDX tumor samples were chosen based on verified *HER2* gene amplification (Supplementary Table S2), and tucatinib was evaluated alone or in combination with trastuzumab and compared with trastuzumab as a single agent.

Tucatinib as a single agent demonstrated activity in 3 breast (**Fig. 5A**), 3 gastric (**Fig. 5B**), 3 colorectal cancer PDX models (**Fig. 5C**), and 2 esophageal PDX models (**Fig. 5D**); %TGI values are

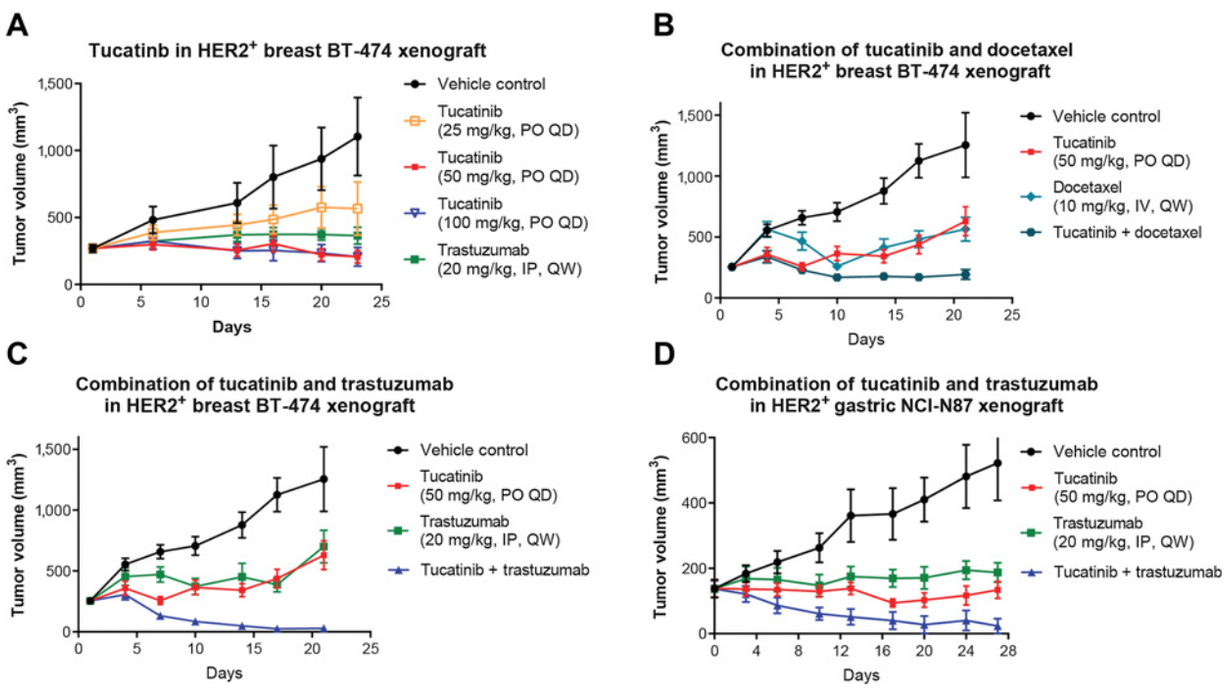

Figure 4.

Tucatinib monotherapy or in combination with trastuzumab or docetaxel reduces tumor volume in HER2$^+$ breast and gastric CDX xenograft models. CDX xenograft models were developed from HER2$^+$ BT-474 breast carcinoma cells (**A–C**) and NCI-N87 gastric carcinoma cells (**D**) and implanted subcutaneously into immunocompromised mice. **A,** Animals ($n = 12$) were treated with increasing doses of tucatinib at the indicated doses for 21 days or with trastuzumab as monotherapy, as indicated, for 21 days. **B,** Animals ($n = 12$) were treated with tucatinib, docetaxel, the combination of tucatinib + docetaxel, or vehicle, as indicated, for 21 days. **C** and **D,** Animals were treated with tucatinib, trastuzumab, the combination of tucatinib + trastuzumab, or vehicle as indicated, for 21 days. Tumor volumes were measured at select timepoints throughout the experiment. Data are reported as MTV ± SEM. PO, orally; QD, every day; QW, once weekly; IP, intraperitoneally.

Downloaded from http://aacrjournals.org/mct/article-pdf/19/4/976/1848445/976.pdf by guest on 19 May 2025

Table 1. *In vivo* efficacy of tucatinib as monotherapy or in combination with trastuzumab in various tumor models.

		Percent tumor growth inhibition (%TGI)			Tumor response rate				
Tumor name	Cancer type	Tucatinib	Trastuzumab	Tucatinib + trastuzumab	Tucatinib	Trastuzumab	Tucatinib + trastuzumab	Animals per arm (*n*)	Number of days of treatment
BT-474	Breast carcinoma CDX	86	68	133	0	0	1 PR; 10 CR	12	21
NCI-N87	Gastric carcinoma CDX	101	87	130	4 PR	0	7 PR; 2 CR	10	21
CTG-0708	Breast carcinoma PDX	88	66	98	0	0	0	8	28
CTG-0717	Breast carcinoma PDX	79	21	99	1 PR	0	3 PR	8	28
CTG-0807	Breast carcinoma PDX	98	63	120	2 PR	0	6 PR	8	28
CTG-0121	Colorectal carcinoma PDX	104	109	124	6 PR	8 PR	10 PR	10	28
CTG-0383	Colorectal carcinoma PDX	117	80	137	6 PR	4 PR	10 PR	10	28
CTG-0784	Colorectal carcinoma PDX	50	36	103	1 PR	0	0	10	28
CTG-0137	Esophageal carcinoma PDX	49	55	85	0	0	0	10	28
CTG-0138	Esophageal carcinoma PDX	69	−34	120	2 PR	0	9 PR	10	28
GXA-3038	Gastric carcinoma PDX	110	50	116	6 PR; 3CR	0	5 PR; 5 CR	10	28
GXA-3039	Gastric carcinoma PDX	48	38	103	0	0	2 PR; 1 CR	7	28
GXA-3054	Gastric carcinoma PDX	65	93	136	1 PR	4 PR; 3 CR	3 PR; 7 CR	10	28

Note: %TGI was calculated as [1 - (MTV in treatment group on day X - MTV in treatment group on day 0)/(MTV in vehicle group on day X - MTV in vehicle group on day 0)]. %TGI was typically calculated 0 to 2 days after the last day of tucatinib dosing, except for BT-474, CTG-0137, and CTG-0708 where %TGI was calculated on day 14, 15, and 24, respectively, due to rapid tumor growth in the vehicle group and animal sacrifices mandated by the protocol. Tumor regression criteria: PR > 30% reduction in tumor volume at time of first treatment for at least 2 consecutive measurements; CR, no detectable tumor for at least 2 consecutive measurements.

listed in **Table 1**. In each of these models, the MTV of the combination of tucatinib + trastuzumab was significant relative to the vehicle group, and was more active than either drug alone in multiple tumor models (summarized in **Table 1**). In two of the breast cancer PDX models, tucatinib + trastuzumab resulted in superior tumor growth inhibition (**Fig. 5A**) compared with trastuzumab alone (CTG-0708, $P = 0.0431$; CTG-0717, $P = 0.0243$) with partial responses noted in the CTG-0717 and CTG-0807 models (**Table 1**). Importantly, each of these breast PDX models are derived from patients that had shown clinical disease progression with trastuzumab combination regimens.

In the gastric tumor xenograft experiments (**Fig. 5B**), tucatinib in combination with trastuzumab produced a higher number of partial and complete tumor regressions compared with either monotherapy alone (**Table 1**). In the GXA-3038 model, tucatinib alone was more active than trastuzumab alone ($P = 0.0072$) and the combination of tucatinib with trastuzumab was also significantly more active than trastuzumab alone ($P = 0.0017$). In the GXA-3039 model, the combination of tucatinib and trastuzumab was significantly more active than tucatinib alone ($P = 0.0006$) or trastuzumab alone ($P < 0.0001$).

In the colorectal PDX models, tucatinib and trastuzumab treatment significantly reduced MTVs compared with vehicle among colorectal tumor xenograft experiments (**Fig. 5C**) and the combination of both drugs produced higher partial tumor regressions in 2 of 3 colorectal models (**Table 1**). In the CTG-0383 model, the combination of tucatinib with trastuzumab was significantly more active than trastuzumab alone ($P = 0.0280$). Likewise, the combination of tucatinib with trastuzumab was significantly more active than trastuzumab alone ($P = 0.030$) in the CTG-0784 colorectal model.

In the esophageal PDX models, tucatinib + trastuzumab treatment significantly reduced MTVs compared with vehicle (**Fig. 5D**) and induced tumor regressions in CTG-0138 model (**Table 1**). In the CTG-0137 model, the combination of tucatinib and trastuzumab was significantly more active than tucatinib monotherapy ($P = 0.0027$) or trastuzumab monotherapy ($P = 0.0117$). In the CTG-0138 model, tucatinib monotherapy was more effective than trastuzumab monotherapy ($P = 0.003$) and the combination of tucatinib and trastuzumab was also significantly more active than trastuzumab monotherapy ($P < 0.0001$; **Fig. 5D**; **Table 1**). In total, these data, together with the results in breast and gastric CDX xenograft models, support the idea that tucatinib is active as single agent in diverse HER2$^+$ solid tumor models and that the combination of tucatinib with trastuzumab can enhance antitumor responses in many of these models.

Treatment of mice with tucatinib or the combination of tucatinib with trastuzumab was well tolerated with net positive weight gain over the course of the studies and similar to vehicle or trastuzumab single-agent treatment in many models (Supplementary Fig. S2).

Discussion

The advent of HER2-targeted therapies has resulted in a dramatic improvement in the survival of patients with HER2$^+$ breast cancer. In addition to breast cancer, other HER2$^+$ cancers, including gastric and colorectal, have been shown to respond to combination therapies that include HER2-targeted agents (5, 9, 10, 34). However, despite the effectiveness of these therapeutic strategies, there remains a need for new HER2-targeted therapies. The data presented here demonstrate that tucatinib is a novel, highly selective, and potent HER2-targeted TKI that exhibits activity in a variety of HER2$^+$ cancer models.

Biochemical assays demonstrate that tucatinib is a selective inhibitor of HER2 enzymatic activity, with reduced potency against EGFR.

Downloaded from http://aacrjournals.org/mct/article-pdf/19/4/976/1848445/976.pdf by guest on 19 May 2025

This property distinguishes tucatinib from other HER2-targeted TKIs, including lapatinib and neratinib, which are potent inhibitors of both HER2 and EGFR (22, 23). In a broad kinome screen, it was shown that tucatinib potently targets only members of the EGFR RTK family when tested at drug concentrations that are 100- or 1,000-fold the biochemical IC_{50} value for HER2 kinase inhibition. Similar selectivity for the EGFR kinase family was demonstrated with lapatinib, a structurally similar kinase inhibitor, but the HER2/EGFR inhibitor neratinib

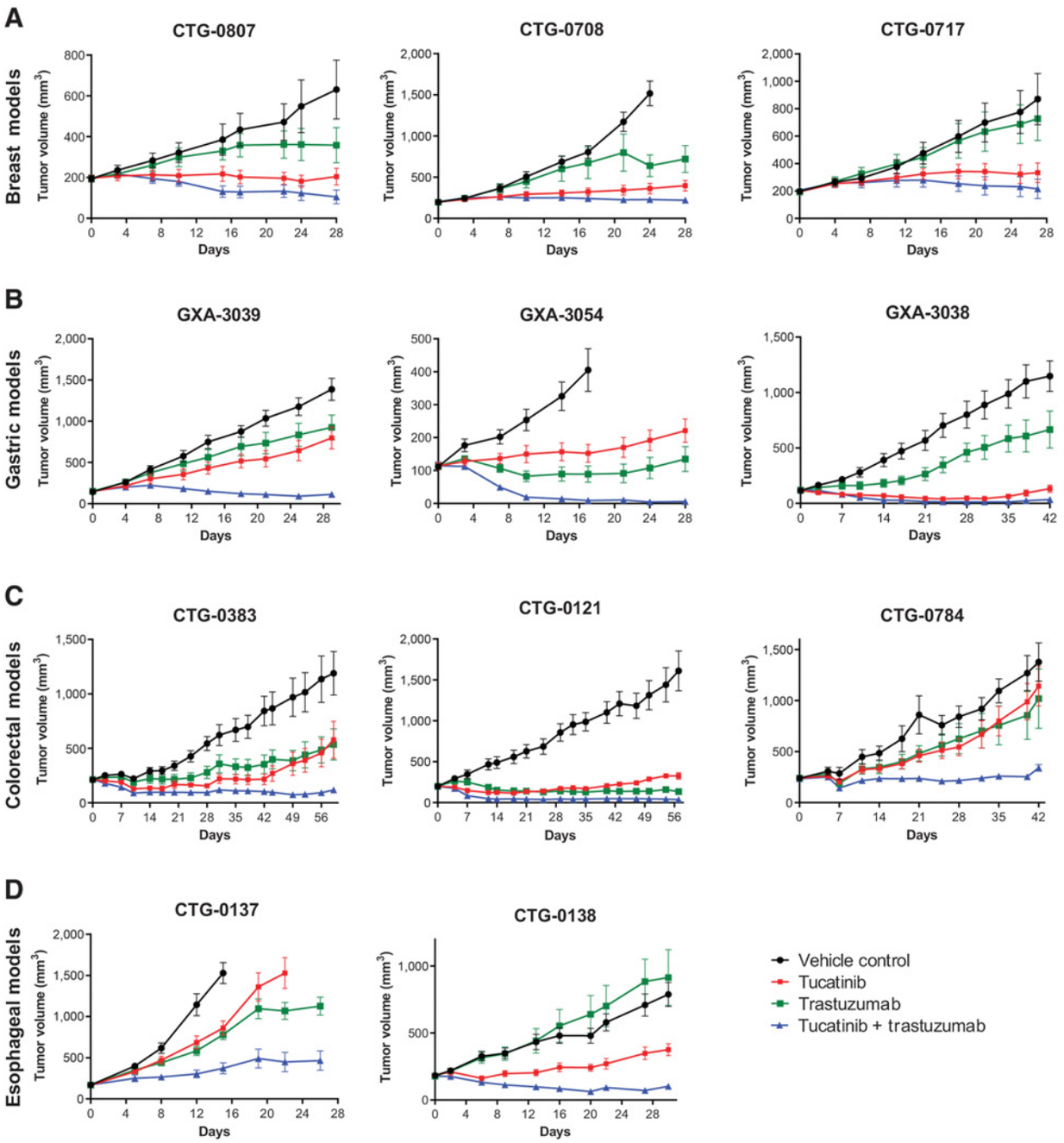

Figure 5.

Tucatinib monotherapy or in combination with trastuzumab significantly reduces tumor volume in $HER2^+$ breast, gastric, colorectal, and esophageal PDX xenograft models. PDX xenograft models were developed from $HER2^+$ breast (**A**), gastric (**B**), colorectal (**C**), and esophageal cancers. **D,** Tumor fragments implanted subcutaneously into the flank of female nude mice. Animals were treated with tucatinib (50 mg/kg, orally, twice a day), trastuzumab (20 mg/kg, intraperitoneally, every 3 days [gastric, colorectal, and esophageal) or once weekly (breast)], the combination of tucatinib + trastuzumab, or vehicle. Dosing continued for 28 days and tumor volume measurements were followed for up to 60 days after treatment initiation. Tumor volumes were measured at select timepoints throughout the experiment. Data are reported as MTV ± SEM.

Downloaded from http://aacrjournals.org/mct/article-pdf/19/4/976/1848445/976.pdf by guest on 19 May 2025

demonstrated a much higher degree of promiscuity in kinome profiling, which may be a property of the covalent-binding mechanism of action (35).

The biological relevance of the HER2 selectivity of tucatinib was demonstrated when measured using tumor-derived cell lines containing HER2 or EGFR amplification. In HER2-amplified BT-474 cells, tucatinib blocked HER2 phosphorylation with an IC_{50} of 7 nmol/L, but at drug concentrations up to 10 μmol/L, there was no reduction in EGFR phosphorylation in EGFR-amplified A431 cells. This result was distinct from both lapatinib and neratinib, which potently inhibited both HER2 and EGFR phosphorylation in these two cell lines. Similar results were demonstrated using the NCI-N87 HER2$^+$ gastric cancer cell line, with tucatinib producing potent inhibition of HER2 phosphorylation with only a modest reduction in EGFR phosphorylation at 1 μmol/L drug. In contrast, lapatinib and neratinib potently inhibited both HER2 and EGFR phosphorylation in the NCI-N87 line. These results are consistent with published data on lapatinib and neratinib. For example, lapatinib showed equivalent potency for inhibiting HER2 and EGFR in enzymatic and cell signaling assays and demonstrated similar potencies in blocking proliferation of either BT-474 or A431 cells *in vitro* (22). Likewise, neratinib also demonstrates similar inhibitory potencies in enzymatic assays comparing HER2 and EGFR, and in cell signaling assays for HER2 (BT-474 cells) and EGFR (A431 cells; ref. 23).

The enhancement in the relative potency for HER2 compared with EGFR in cell signaling assays (>1,000-fold) compared with enzymatic assays (≈50-fold) may reflect differences in the structure of the ATP-binding pocket of the kinase domain of fully processed and plasma membrane–localized enzymes compared with the recombinant proteins used in enzymatic assays. Differences in enzymatic and cellular potencies within the EGFR family have been observed previously. Characterization of the covalent HER2 inhibitor TAS0728 showed only a 5-fold difference in IC_{50} values between HER2 and EGFR in biochemical assays using recombinant material, but cellular HER2 (SK-BR-3 cells) and EGFR (A431 cells) assays showed much greater selectivity for the inhibition of HER2 compared with EGFR (36). Consistent with the increased potency for HER2 inhibition in signaling assays, TAS0728 also showed a more potent IC_{50} value for BT-474 cells (3.6 nmol/L) than for A431 cells (450 nmol/L) in proliferation assays (36).

The capacity of tucatinib to block HER2 phosphorylation in the BT-474 cells is associated with potent inhibition of cell proliferation. The half-maximal tucatinib concentrations for HER2 kinase inhibition were proportional to the cytotoxic IC_{50} value. Likewise, the reduced cytotoxicity IC_{50} value in A431 cells is consistent with the lack of EGFR kinase inhibition observed in these cells. The selectivity of tucatinib for HER2 is further supported by the data showing that the cytotoxic activity of tucatinib correlated with HER2 expression levels in a panel of breast cancer cell lines; only HER2-amplified cell lines showed a high degree of sensitivity to tucatinib.

The ability of tucatinib to potently inhibit cell proliferation in HER2$^+$ breast cancer cell lines is consistent with the cell signaling data that demonstrate the inhibition of key prosurvival and mitogenic signaling, including a blockade of HER3 phosphorylation, inhibition of AKT phosphorylation at serine 473, and inhibition of phosphorylation of ERK1/2 at threonine 185 and 187, and MEK1 at serine 222. The combination of tucatinib + trastuzumab resulted in more complete inhibition of AKT phosphorylation and enhanced apoptosis in BT-474 cells. These data are consistent with recently published results (37) and suggest that the complementary action of tucatinib + trastuzumab on HER2 signaling results in a more effective blockade of cell survival signaling.

There is strong evidence for single-agent antitumor activity of tucatinib across a variety of HER2$^+$ tumor models. In multiple tumor models, tucatinib alone resulted in tumor regressions. These data are consistent with the findings from the phase-I clinical trial results with tucatinib as a single agent, where it was demonstrated that in patients with HER2$^+$ solid tumors ($n = 35$), tucatinib produced an objective response rate (ORR) of 9% (19); in an expansion cohort of patients with HER2$^+$ MBC ($n = 22$) treated with higher doses of tucatinib, the ORR was 14%, all of which were PRs (19).

The increased activity of dual targeting of HER2, either through combinations of two different HER2-targeted antibodies or by use of a HER2-targeted antibody and TKI, has been shown to improve outcomes in preclinical studies and in patients with HER2$^+$ cancers (10, 38). In this study, the combinatorial activity of tucatinib + trastuzumab also produced improved antitumor activity *in vivo* in HER2$^+$ CDX and PDX xenograft models of breast, gastric, colorectal, and esophageal cancers. Overall, there were substantially more partial and complete tumor regressions induced by tucatinib + trastuzumab combination therapy compared with either single agent alone. Across the CDX and PDX models, there were 25 complete tumor regressions; induced by the combination of tucatinib + trastuzumab, compared with 3 generated by tucatinib and 3 by trastuzumab alone. The overall regression rate for tucatinib in these studies was 26%, with a 15% regression rate for trastuzumab and a 66% regression rate for the combination of both agents.

These preclinical data support the contention that tucatinib is a potent HER2-selective TKI and that the selective inhibition of HER2 signal can drive robust antitumor activity across multiple models of HER2$^+$ cancer. In particular, these results highlight the utility of combining tucatinib + trastuzumab, which may translate to produce enhanced clinical activity. These preclinical results and early clinical data support the hypothesis that selective inhibition of HER2 activity by tucatinib, in the absence of EGFR inhibition, can be an effective therapeutic approach in HER2$^+$ cancers. This is an important point since currently available small-molecule TKI therapies for HER2$^+$ breast cancer are equipotent HER2 and EGFR inhibitors, and are associated with skin and gastrointestinal toxicities that may reduce patient quality-of-life (24, 25, 39–43). Although EGFR is expressed in HER2$^+$ cancers (44), the role of EGFR expression in the outcome of metastatic patients treated with trastuzumab regimens is unclear (45). Similarly, the therapeutic benefit of inhibiting EGFR in HER2$^+$ MBC has not been clearly defined. For example, in a phase I–II study of the combination of trastuzumab and gefitinib (an EGFR-targeted TKI) in HER2$^+$ MBC, 250 or 500 mg/day doses of gefitinib were tested together with trastuzumab (46). All patients treated with the 500 mg/day dose of gefitinib developed grade 3/4 gastrointestinal toxicity and that dose combination was deemed beyond the MTD. At the tolerated dose of 250 mg/day, there was an ORR of 9% and a clinical benefit rate of 28%. An interim analysis of this trial indicated that the 250 mg gefitinib/trastuzumab combination did not merit further testing. These data also suggest that the potent inhibition of EGFR with dual EGFR/HER2 inhibitors could reduce drug tolerability and potentially restrict HER2 target saturation.

In summary, we have demonstrated that tucatinib is a potent and highly selective HER2 kinase inhibitor with increased selectivity for HER2 compared with earlier-generation HER2-targeted TKIs such as lapatinib and neratinib. Pharmacologic data from both *in vitro* and *in vivo* studies demonstrate that tucatinib has antitumor activity, both as a single agent and in combination with either

Downloaded from http://aacrjournals.org/mct/article-pdf/19/4/976/1848445/976.pdf by guest on 19 May 2025

docetaxel or trastuzumab. These characteristics are consistent with tucatinib's observed safety and activity in early clinical trials in patients with HER2$^+$ MBC, including the phase I ONT-380-005 study (NCT02025192) in combination with trastuzumab or trastuzumab and capecitabine (26) and the phase I ONT-380-004 study (NCT01983501) combining tucatinib with Ado-Trastuzumab Emtansine in patients with HER2$^+$ MBC with or without brain metastases (28). Furthermore, the outcome of an international, randomized, double-blind trial comparing the combination of tucatinib plus trastuzumab and capecitabine to placebo plus trastuzumab and capecitabine was recently reported (47). The results of this trial demonstrated the addition of tucatinib to trastuzumab and capecitabine resulted in better progression-free survival and overall survival outcomes in patients with heavily pretreated HER2-positive MBC, including those with brain metastases. These clinical results, together with the preclinical data described in this article, support the clinical evaluation of tucatinib in additional HER2$^+$ cancers, including colorectal, esophageal, and gastric cancers.

Disclosure of Potential Conflicts of Interest

A. Kulukian is a senior scientist and has ownership interest (including patents) in Seattle Genetics. P. Lee is a vice president, pharmacology/toxicology at Array BioPharma. J. Taylor is a staff scientist and has ownership interest (including patents) at Seattle Genetics. A. Forero-Torres is an executive medical director at Seattle Genetics. S. Peterson is a vice president, reports receiving a commercial research grant, and has ownership interest (including patents) in Seattle Genetics. No potential conflicts of interest were disclosed by the other authors.

Authors' Contributions

Conception and design: A. Kulukian, S. Peterson
Development of methodology: A. Kulukian, P. Lee, R. Rosler, S. Peterson
Acquisition of data (provided animals, acquired and managed patients, provided facilities, etc.): A. Kulukian, P. Lee, J. Taylor, R. Rosler, S. Peterson
Analysis and interpretation of data (e.g., statistical analysis, biostatistics, computational analysis): A. Kulukian, P. Lee, J. Taylor, R. Rosler, P. de Vries, A. Forero-Torres, S. Peterson
Writing, review, and/or revision of the manuscript: A. Kulukian, P. Lee, J. Taylor, R. Rosler, A. Forero-Torres, S. Peterson
Administrative, technical, or material support (i.e., reporting or organizing data, constructing databases): A. Kulukian, P. Lee, P. de Vries, D. Watson, S. Peterson
Study supervision: A. Kulukian, P. Lee, P. de Vries, S. Peterson

Acknowledgments

Medical writing and editing assistance was provided by Michael R. Convente, Ph.D. (ScientificPathways, Inc.) with funding from Seattle Genetics, Inc. Production of the tucatinib kinome tree was provided by Robert Thurman, Ph.D. (Seattle Genetics). The experiments described in this manuscript were funded by Seattle Genetics.

The costs of publication of this article were defrayed in part by the payment of page charges. This article must therefore be hereby marked *advertisement* in accordance with 18 U.S.C. Section 1734 solely to indicate this fact.

Received September 12, 2019; revised November 26, 2019; accepted February 18, 2020; published first April 1, 2020.

Downloaded from http://aacrjournals.org/mct/article-pdf/19/4/976/1848445/976.pdf by guest on 19 May 2025

References

1. Hynes NE, Lane HA. ERBB receptors and cancer: the complexity of targeted inhibitors. Nat Rev Cancer 2005;5:341–54.
2. Moasser MM. The oncogene HER2: its signaling and transforming functions and its role in human cancer pathogenesis. Oncogene 2007;26:6469–87.
3. Vu T, Claret FX. Trastuzumab: updated mechanisms of action and resistance in breast cancer. Front Oncol 2012;2:62.
4. Du Z, Lovly CM. Mechanisms of receptor tyrosine kinase activation in cancer. Mol Cancer 2018;17:58.
5. Gerson JN, Skariah S, Denlinger CS, Astsaturov I. Perspectives of HER2-targeting in gastric and esophageal cancer. Expert Opin Investig Drugs 2017; 26:531–40.
6. Witton CJ, Reeves JR, Going JJ, Cooke TG, Bartlett JM. Expression of the HER1-4 family of receptor tyrosine kinases in breast cancer. J Pathol 2003;200:290–7.
7. Slamon DJ, Clark GM, Wong SG, Levin WJ, Ullrich A, McGuire WL. Human breast cancer: correlation of relapse and survival with amplification of the HER-2/neu oncogene. Science 1987;235:177–82.
8. Koninki K, Tanner M, Auvinen A, Isola J. HER-2 positive breast cancer: decreasing proportion but stable incidence in Finnish population from 1982 to 2005. Breast Cancer Res 2009;11:R37.
9. Boku N. HER2-positive gastric cancer. Gastric Cancer 2014;17:1–12.
10. Sartore-Bianchi A, Trusolino L, Martino C, Bencardino K, Lonardi S, Bergamo F, et al. Dual-targeted therapy with trastuzumab and lapatinib in treatment-refractory, KRAS codon 12/13 wild-type, HER2-positive metastatic colorectal cancer (HERACLES): a proof-of-concept, multicentre, open-label, phase 2 trial. Lancet Oncol 2016;17:738–46.
11. Shi F, Telesco SE, Liu Y, Radhakrishnan R, Lemmon MA. ErbB3/HER3 intracellular domain is competent to bind ATP and catalyze autophosphorylation. Proc Natl Acad Sci U S A 2010;107:7692–7.
12. Sachdev JC, Jahanzeb M. Blockade of the HER family of receptors in the treatment of HER2-positive metastatic breast cancer. Clin Breast Cancer 2012;12:19–29.
13. Ruiz-Saenz A, Dreyer C, Campbell MR, Steri V, Gulizia N, Moasser MM. HER2 amplification in tumors activates PI3K/Akt signaling independent of HER3. Cancer Res 2018;78:3645–58.
14. Luque-Cabal M, Garcia-Teijido P, Fernandez-Perez Y, Sanchez-Lorenzo L, Palacio-Vazquez I. Mechanisms behind the resistance to trastuzumab in HER2-amplified breast cancer and strategies to overcome it. Clin Med Insights Oncol 2016;10:21–30.
15. Gianni L, Pienkowski T, Im YH, Tseng LM, Liu MC, Lluch A, et al. 5-year analysis of neoadjuvant pertuzumab and trastuzumab in patients with locally advanced, inflammatory, or early-stage HER2-positive breast cancer (NeoSphere): a multicentre, open-label, phase 2 randomised trial. Lancet Oncol 2016;17:791–800.
16. Chan A, Delaloge S, Holmes FA, Moy B, Iwata H, Harvey VJ, et al. Neratinib after trastuzumab-based adjuvant therapy in patients with HER2-positive breast cancer (ExteNET): a multicentre, randomised, double-blind, placebo-controlled, phase 3 trial. Lancet Oncol 2016;17:367–77.
17. von Minckwitz G, Procter M, de Azambuja E, Zardavas D, Benyunes M, Viale G, et al. Adjuvant pertuzumab and trastuzumab in early HER2-positive breast cancer. N Engl J Med 2017;377:122–31.
18. Earl HM, Hiller L, Vallier AL, Loi S, McAdam K, Hughes-Davies L, et al. 6 versus 12 months of adjuvant trastuzumab for HER2-positive early breast cancer (PERSEPHONE): 4-year disease-free survival results of a randomised phase 3 non-inferiority trial. Lancet 2019;393:2599–612.
19. Moulder SL, Borges VF, Baetz T, McSpadden T, Fernetich G, Murthy RK, et al. Phase I study of ONT-380, a HER2 inhibitor, in patients with HER2 (+)-advanced solid tumors, with an expansion cohort in HER2(+) metastatic breast cancer (MBC). Clin Cancer Res 2017;23:3529–36.
20. Venur VA, Leone JP. Targeted therapies for brain metastases from breast cancer. Int J Mol Sci 2016;17.
21. Wong AL, Lee SC. Mechanisms of resistance to trastuzumab and novel therapeutic strategies in HER2-positive breast cancer. Int J Breast Cancer 2012;2012: 415170.
22. Rusnak DW, Lackey K, Affleck K, Wood ER, Alligood KJ, Rhodes N, et al. The effects of the novel, reversible epidermal growth factor receptor/ErbB-2 tyrosine kinase inhibitor, GW2016, on the growth of human normal and tumor-derived cell lines *in vitro* and *in vivo*. Mol Cancer Ther 2001;1:85–94.
23. Rabindran SK, Discafani CM, Rosfjord EC, Baxter M, Floyd MB, Golas J, et al. Antitumor activity of HKI-272, an orally active, irreversible inhibitor of the HER-2 tyrosine kinase. Cancer Res 2004;64:3958–65.
24. Frankel C, Palmieri FM. Lapatinib side-effect management. Clin J Oncol Nurs 2010;14:223–33.

25. Sodergren SC, Copson E, White A, Efficace F, Sprangers M, Fitzsimmons D, et al. Systematic review of the side effects associated with anti-HER2-targeted therapies used in the treatment of breast cancer, on behalf of the EORTC quality of life group. Target Oncol 2016;11:277–92.
26. Murthy R, Borges VF, Conlin A, Chaves J, Chamberlain M, Gray T, et al. Tucatinib with capecitabine and trastuzumab in advanced HER2-positive metastatic breast cancer with and without brain metastases: a non-randomised, open-label, phase 1b study. Lancet Oncol 2018;19:880–8.
27. Pheneger T, Bouhana K, Anderson D, Garrus J, Ahrendt K, Allen S, et al. *In vitro* and *in vivo* activity of ARRY-380: a potent, small molecule inhibitor of ErbB2 [abstract]. In: Proceedings of the Thirty-Second Annual CTRCAACR San Antonio Breast Cancer Symposium; 2009 Dec 10-13; San Antonio, TX. Philadelphia (PA): AACR; 2009. Abstract nr 5104.
28. Borges VF, Ferrario C, Aucoin N, Falkson C, Khan Q, Krop I, et al. Tucatinib combined with ado-trastuzumab emtansine in advanced ERBB2/HER2-positive metastatic breast cancer: a phase 1b clinical trial. JAMA Oncol 2018;4:1214–20.
29. Eid S, Turk S, Volkamer A, Rippmann F, Fulle S. KinMap: a web-based tool for interactive navigation through human kinome data. BMC Bioinformatics 2017;18:16.
30. Szollosi J, Balazs M, Feuerstein BG, Benz CC, Waldman FM. ERBB-2 (HER2/neu) gene copy number, p185HER-2 overexpression, and intratumor heterogeneity in human breast cancer. Cancer Res 1995;55:5400–7.
31. Merlino GT, Xu YH, Ishii S, Clark AJ, Semba K, Toyoshima K, et al. Amplification and enhanced expression of the epidermal growth factor receptor gene in A431 human carcinoma cells. Science 1984;224:417–9.
32. Ghosh R, Narasanna A, Wang SE, Liu S, Chakrabarty A, Balko JM, et al. Trastuzumab has preferential activity against breast cancers driven by HER2 homodimers. Cancer Res 2011;71:1871–82.
33. Lyseng-Williamson KA, Fenton C. Docetaxel: a review of its use in metastatic breast cancer. Drugs 2005;65:2513–31.
34. Meric-Bernstam F, Hurwitz H, Raghav KPS, McWilliams RR, Fakih M, VanderWalde A, et al. Pertuzumab plus trastuzumab for HER2-amplified metastatic colorectal cancer (MyPathway): an updated report from a multicentre, open-label, phase 2a, multiple basket study. Lancet Oncol 2019;20:518–30.
35. Davis MI, Hunt JP, Herrgard S, Ciceri P, Wodicka LM, Pallares G, et al. Comprehensive analysis of kinase inhibitor selectivity. Nat Biotechnol 2011;29:1046–51.
36. Irie H, Ito K, Fujioka Y, Oguchi K, Fujioka A, Hashimoto A, et al. TAS0728, a covalent-binding, HER2-selective kinase inhibitor shows potent antitumor activity in preclinical models. Mol Cancer Ther 2019;18:733–42.
37. Schwill M, Tamaskovic R, Gajadhar AS, Kast F, White FM, Pluckthun A. Systemic analysis of tyrosine kinase signaling reveals a common adaptive response program in a HER2-positive breast cancer. Sci Signal 2019;12.
38. Xu ZQ, Zhang Y, Li N, Liu PJ, Gao L, Gao X, et al. Efficacy and safety of lapatinib and trastuzumab for HER2-positive breast cancer: a systematic review and meta-analysis of randomised controlled trials. BMJ Open 2017;7:e013053.
39. Lacouture ME, Laabs SM, Koehler M, Sweetman RW, Preston AJ, Di Leo A, et al. Analysis of dermatologic events in patients with cancer treated with lapatinib. Breast Cancer Res Treat 2009;114:485–93.
40. Friedman MD, Lacouture M, Dang C. Dermatologic adverse events associated with use of adjuvant lapatinib in combination with paclitaxel and trastuzumab for HER2-positive breast cancer: a case series analysis. Clin Breast Cancer 2016;16:e69–74.
41. Lacouture ME, Schadendorf D, Chu CY, Uttenreuther-Fischer M, Stammberger U, O'Brien D, et al. Dermatologic adverse events associated with afatinib: an oral ErbB family blocker. Expert Rev Anticancer Ther 2013;13:721–8.
42. Harandi A, Zaidi AS, Stocker AM, Laber DA. Clinical efficacy and toxicity of anti-EGFR therapy in common cancers. J Oncol 2009;2009:567486.
43. Dang C, Lin N, Moy B, Come S, Sugarman S, Morris P, et al. Dose-dense doxorubicin and cyclophosphamide followed by weekly paclitaxel with trastuzumab and lapatinib in HER2/neu-overexpressed/amplified breast cancer is not feasible because of excessive diarrhea. J Clin Oncol 2010;28:2982–8.
44. DiGiovanna MP, Stern DF, Edgerton SM, Whalen SG, Moore D II, Thor AD. Relationship of epidermal growth factor receptor expression to ErbB-2 signaling activity and prognosis in breast cancer patients. J Clin Oncol 2005;23:1152–60.
45. Lee HJ, Seo AN, Kim EJ, Jang MH, Kim YJ, Kim JH, et al. Prognostic and predictive values of EGFR overexpression and EGFR copy number alteration in HER2-positive breast cancer. Br J Cancer 2015;112:103–11.
46. Arteaga CL, O'Neill A, Moulder SL, Pins M, Sparano JA, Sledge GW, et al. A phase I-II study of combined blockade of the ErbB receptor network with trastuzumab and gefitinib in patients with HER2 (ErbB2)-overexpressing metastatic breast cancer. Clin Cancer Res 2008;14:6277–83.
47. Murthy RK, Loi S, Okines A, Paplomata E, Hamilton E, Hurvitz SA, et al. Tucatinib, trastuzumab, and capecitabine for HER2-positive metastatic breast cancer. N Engl J Med 2020;382:597–609.

Downloaded from http://aacrjournals.org/mct/article-pdf/19/4/976/1848445/976.pdf by guest on 19 May 2025